CHEMISTRY OF MATERIALS

ARTICLE

pubs.acs.org/cm

Metallo-Responsive Liquid Crystalline Monomers and Polymers

Blayne M. McKenzie,[†] Rudy J. Wojtecki,[†] Kelly A. Burke,[†] Cuiyu Zhang,[‡] Antal Jákli,[‡] Patrick T. Mather,[§] and Stuart J. Rowan[†,*]

[†]Department of Macromolecular Science and Engineering, Case Western Reserve University, 2100 Adelbert Road, Cleveland, Ohio 44106-7202, United States

[‡]Liquid Crystal Institute, Kent State University, Kent, Ohio 44240, United States

[§]Department of Biomedical and Chemical Engineering, Syracuse University, Syracuse, New York 13244, United States

Supporting Information

ABSTRACT: A series of liquid crystalline ligand-containing monomers with chemo-responsive properties has been prepared and studied. These molecules are functionalized derivatives of the 2,6-bisbenzimidazolylpyridine (Bip) ligand. Tailoring the size of the aromatic core and the length of two pairs of alkyl substituents allows the preparation of mesogens with a range of tunable thermal liquid crystalline transitions and phases. The binding of lanthanide- and/or transition metal salts to the ligand containing mesogens results in a transition from a liquid crystalline to an isotropic state. Acyclic diene metathesis of the monomers yielded either oligomers or polymers, dictated by whether the alkene is either terminal or nonterminal, respectively. Both oligomers and polymers exhibit enantiotropic liquid crystalline behavior and become isotropic in the presence of metal ions.

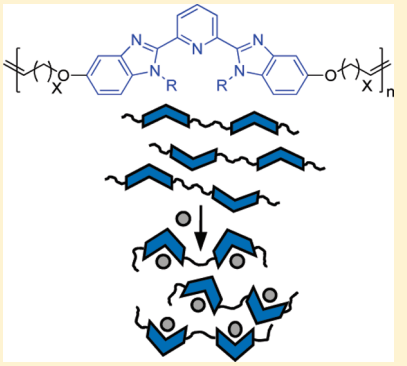

KEYWORDS: ADMET, lanthanides, liquid crystal, stimuli-responsive, supramolecular

INTRODUCTION

Small molecule and polymeric liquid crystalline materials have applications in a multitude of areas, ranging from displays, optical/electronic imaging, data storage, and stress/temperature sensing to chemical/fire resistance and artificial muscle actuation.[1] The design of typical molecular architectures that facilitate thermotropic liquid crystalline behavior is well documented. Molecules with structural anisotropy, i.e., a rigid moiety with high aspect ratio are frequently utilized to impart the order inherent in a liquid crystalline phase. Functionalization of these cores with flexible alkane chains of varying length then provides the structural complexity necessary to hinder crystallization while preserving liquid crystalline order. As such, thermotropic liquid crystals are inherently stimuli-responsive, as they can undergo a range of thermally induced transitions between glassy/crystalline, liquid crystalline, and isotropic states. Examples of thermotropic liquid crystalline small molecules or polymers that are also designed to respond to specific chemical stimuli are less prevalent.[2]

One approach to designing a chemo-responsive liquid crystal involves incorporating a metal-binding ligand into the mesogenic core. In addition to introducing additional, nonthermal, stimuli-responsive behavior incorporation of metal ions into liquid crystalline materials offers the opportunity to impart a number of additional properties upon these systems. Chemical sensing,[3] catalysis,[4] and a host of biological applications[5] highlight the many practical properties of organic metal-coordinating species, while some specific lanthanide complexes also exhibit interesting luminescent and paramagnetic properties.[6] Additionally, the vast number of transition and lanthanide metal ions offers a multitude of potential geometries and binding motifs, which can be utilized to design the specific shapes necessary to retain, induce, or otherwise impact liquid crystallinity. This approach enhances the traditional thermotropic liquid crystal in two ways. First, ligands can be envisioned that, upon binding a metal ion, lose their original liquid crystalline order and thus offer a useful method of amplification for detection schemes and other applications.[7] Second, ligands that bind metal ions and retain, change, or acquire liquid crystalline order (metallomesogens) can also be envisaged.[8]

The 2,6-bisbenzimidazolylpyridine (Bip) ligand offers a versatile scaffold from which highly functionalized derivatives can be accessed (e.g., $\mathbf{1}^{\mathbf{Et}}$, Figure 1).[9,10] Piguet and co-workers have prepared a number of low molecular weight mesogenic Bip derivatives and investigated the effects of metal binding on their liquid crystalline properties.[11] Noting that the incorporation of a large metal center disrupts the organization of simpler Bip mesogens,[12] they decorated the Bip core with a highly alkylated liquid crystallinity-enhancing moiety in the 5′ positions, which allowed access to a range of metallomesogens.[13] Upon complexation with a variety of $Ln(NO_3)_3$ salts, this Bip derivative displayed columnar or cubic mesomorphism at elevated temperatures. Further functionalization with the highly alkylated moiety at the N[1′] positions increased the geometric screening of the bulky metal complex, facilitating access to room-temperature columnar metallomesogens.[14] Thus, they have presented a room

Received: April 23, 2011
Revised: June 13, 2011
Published: July 05, 2011

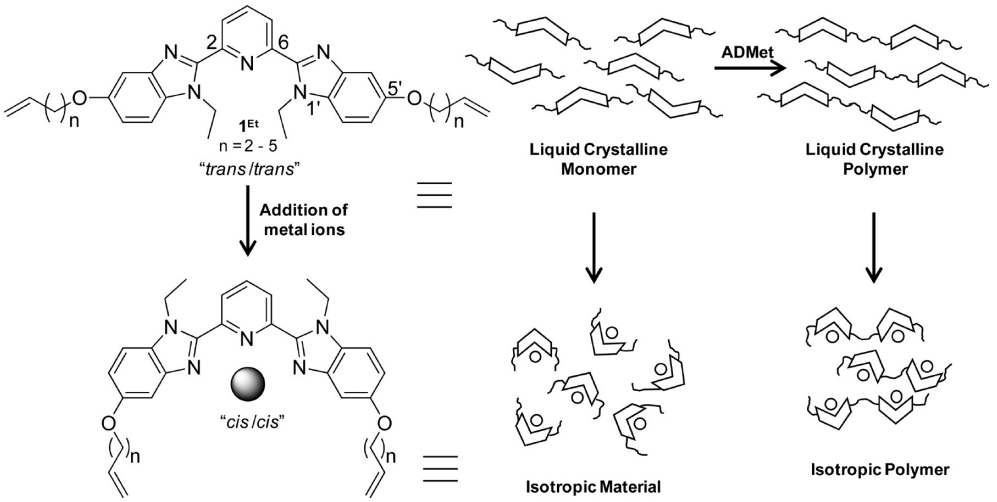

Figure 1. Bip-containing monomer $\mathbf{1}^{\mathbf{Et}}$ in the metal-free "*trans*/*trans*" ligand conformation and 1:1 complex with a metal ion, which adopts the "*cis*/*cis*" ligand conformation, and schematic representations of the polymerization and proposed metallo-response of the monomer and polymer.

temperature "lanthanidomesogen" that balances the structural anisotropy of the Bip core with the fluidity of 12 alkyl chains. Other lanthanidomesogens have been prepared using different binding motifs, such as simple alkyl carboxylates (i.e., lanthanide soaps),[15] porphyrins,[15] and Schiff bases,[15,16] while bipyridine,[17] phenanthroline,[18] terpyridine,[19] and other pyridine-based ligands[20] have been used to prepare metallomesogens with various transition metals.

Our group and others have utilized Bip derivatives to access a range of stimuli-responsive metallo-supramolecular polymers,[21] and we have investigated their potential in a number of material-related areas, from chemical sensors,[22] thermoplastic elastomers,[23] photohealable materials,[24] and stimuli-responsive gels,[25] to processable, robust poly(*p*-xylylene)[26] and poly(*p*-phenylene ethynylene) derivatives.[27] As part of a long-term project to access new stimuli-responsive structurally dynamic polymers,[28] we targeted easy-to-access,[10] mesogenic Bip derivatives (**1**, **2**, Scheme 1) that not only feature relatively low clearing temperatures (75−125 °C), but can also be readily incorporated into polymer and network architectures. In this study, we report the synthesis and liquid crystalline properties of a range of monomeric Bip derivatives that contain alkene functionalities, their behavior in the presence of metal salts, and initial studies in to their polymerization via acyclic diene metathesis chemistry (ADMet).[29]

EXPERIMENTAL SECTION

Materials. All solvents, sodium bicarbonate, potassium carbonate, and potassium hydroxide were purchased from Fisher Scientific. Deuterated solvents were purchased from Norell, Inc. Tetrakis(triphenylphosphine) palladium(0) was purchased from Strem Chemicals, Inc. Grubbs catalyst third generation was prepared via literature procedures and used without further characterization.[30] All other reagents and solvents were purchased from Aldrich Chemical Co. Reagents were used without further purification. Solvents were distilled from suitable drying agents.

Instruments. NMR spectra were recorded on a Varian Inova 600 MHz NMR spectrometer (^{13}C NMR = 150.8 MHz) using deuterated solvents. Molecular weights of the materials were measured on a Bruker AUTOFLEX III MALDI TOF/TOF mass spectrometer using HABA [2-(4-hydroxyphenylazo)benzoic acid] as the matrix. HPLC data were collected using a Varian ProStar with a reverse phase C18 silica analytical column using the following procedure. Flow rate: 1 mL/min; solvent A: H_2O (0.10% trifluoroacetic acid, TFA); solvent B: acetonitrile (MeCN, 0.08% TFA); solvent program: 98% A, 2% B, ramp to 2% A, 98% B over 20 min, hold for 10 min. Elution time was reported as the signal at 365 nm unless otherwise noted. DSC and modulated DSC experiments were performed on a TA Instruments Q2000 DSC equipped with a refrigerated cooling system. The DSC cell resistance and capacitance were calibrated using the Tzero calibration procedure (TA Instruments-Waters LLC), and the cell constant and temperature were calibrated using an indium standard. All samples were run under a flowing nitrogen purge and were heated and cooled at a rate of 10 °C/min. Recrystallization, melting, clearing, and liquid crystalline phase transition temperatures of these monomers were determined from either the peak maxima (for exothermic transitions) or minima (for endothermic transitions) on the second heating or cooling traces. Modulated experiments were heated and cooled at a rate of 3 °C/min, during which a linear heating rate and a sinusoidal temperature waveform were applied to the sample with a modulation amplitude of 1 °C and a modulation period of 30 s. Polarized optical microscopy(POM) studies were performed using an Olympus BX51 microscope equipped with 90° crossed polarizers, an HCS402 hot stage from Instec, Inc., and a digital camera (14.2 Color Mosaic Model from Diagnostic Instruments, Inc.). Images were acquired from the camera at selected temperatures using Spot software (Diagnostic Instruments, Inc.). Spatial dimensions were calibrated using a stage micrometer with 10 μm line spacing. Either a 50x/0.5 NA or a 20x/0.4 NA achromat long working-distance objective lens (Olympus LMPlanFI) was employed. The Instec hotstage was equipped with a liquid nitrogen LN2-P cooling accessory for accurate temperature control during both heating and cooling. Wide-angle X-ray data were acquired on a Rigaku RINT 2000/PC series diffractometer with a Rigaku PTC-30 programmable temperature controller. Photoluminescence spectra were acquired on an Ocean Optics ACD1000-USB spectrometer (λ_{ex} = 377 nm) via a Y-shaped optical fiber. Size exclusion chromatography (SEC) was performed on a Varian ProStar 210/215 equipped with a Varian ProStar 350/352 Refractive Index Detector, a Viscotek Model 270 Dual Detector, and Varian OligoPore and ResiPore SEC/GPC columns running tetrahydrofuran (THF) at a flow rate of 1.0 mL/min.

Synthesis. Compounds **3**, **4a**-**8a**, **4d**, **5d**, and $\mathbf{1}^{\mathbf{Et5}}$ were synthesized according to literature procedures.[10]

Preparation and characterization details of 4-methoxy-*N*-propyl-2-nitroaniline (**4b**), *N*-butyl-4-methoxy-2-nitroaniline (**4c**), 2,6-bis(5′-methoxy-1′-propylbenzimidazol-2′-yl)pyridine (**5b**), 2,6-bis(1′-butyl-5′-methoxybenzimidazol-2′-yl)pyridine (**5c**), 4-bromo-*N*-butyl-2-nitroaniline (**6c**),

dx.doi.org/10.1021/cm2011617 |*Chem. Mater.* 2011, 23, 3525–3533

Scheme 1. Synthesis of Bip-Containing Monomers. (A) Pd(0), K_2CO_3, THF, H_2O, 75 °C, 18 h; (B) (i) DMF, r.t., 12 h; (ii) $Na_2S_2O_4$, DMF, EtOH, H_2O, 85 °C, 12 h; (C) BBr_3, DCM, r.t., 4 h; and (D) $Br(CH_2)_nCH{=}CH_2$, (or $TsO(CH_2)_3CH{=}CHCH_3$) K_2CO_3, THF, MeOH, 75 °C, 12 h

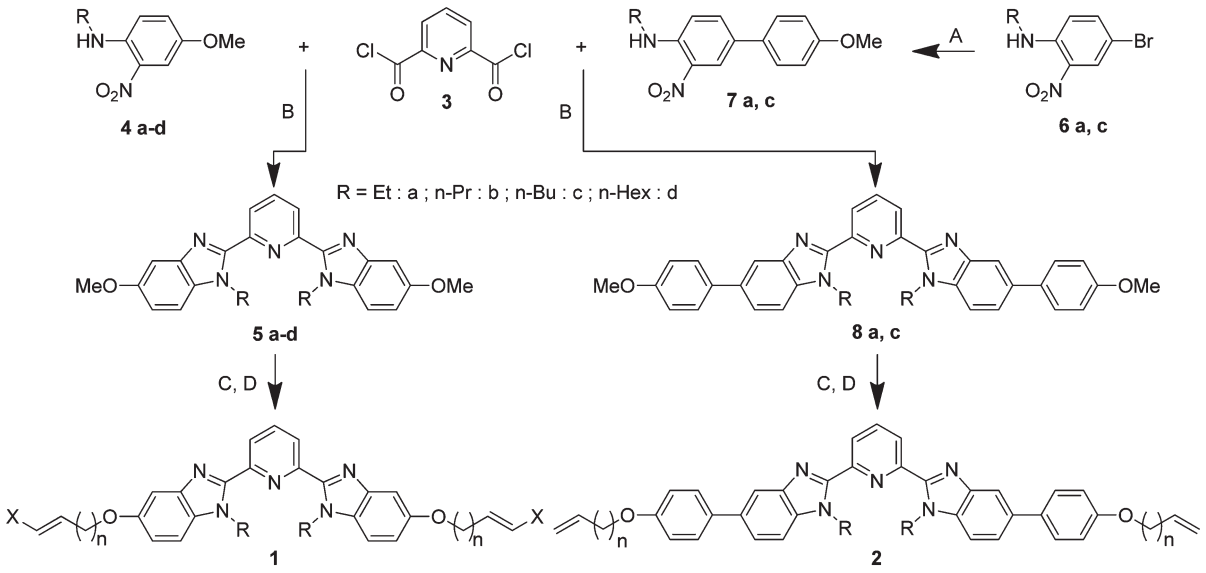

R	n	X		R	n	X	
Et	2	H	$\mathbf{1}^{Et4}$	Et	3	CH_3	$\mathbf{1}^{Et5Me}$
Et	3	H	$\mathbf{1}^{Et5}$	n-Pr	3	H	$\mathbf{1}^{Pr5}$
Et	4	H	$\mathbf{1}^{Et6}$	n-Bu	3	H	$\mathbf{1}^{Bu5}$
Et	5	H	$\mathbf{1}^{Et7}$	n-Hex	3	H	$\mathbf{1}^{Hx5}$
Et	9	H	$\mathbf{1}^{Et11}$	n-Bu	5	H	$\mathbf{1}^{Bu7}$

R	n	
Et	3	$\mathbf{2}^{Et5}$
n-Bu	3	$\mathbf{2}^{Bu5}$

N-butyl-2-nitro-4-(4′-methoxy)phenylaniline (**7c**), and 2,6-bis(1′-butyl-(4″-methoxy)phenylbenzimidazol-2′-yl)pyridine (**8c**) are located in the Supporting Information.

*General Procedure for the Preparation of **1** and **2**.* (C in Scheme 1) The appropriate methoxy derivative (**5** or **8**) was dissolved in dry dichloromethane (DCM, 100 mM) in a round-bottomed flask. The flask was sealed with a septum and flushed with nitrogen (3x). While under nitrogen, boron tribromide (5 equivalents) was added via syringe, and the reaction was stirred for 4 h at room temperature. The contents of the flask were then slowly added to stirring water (1:1 DCM:H_2O) and neutralized to pH ~7 with sodium bicarbonate. The desired phenolic derivative was obtained by filtering the aqueous suspension and drying the solids under vacuum. The following is an example of the characterization data for the phenolic derivative of **5a**. Similar data for the additional derivatives of **5** and **8** are located in the Supporting Information.

*Phenolic Derivative of **5a**.* Precipitated from water to yield the product as an off-white solid (98%); mp: >250 °C (decomp). ^{1}H NMR (600 MHz, CD_3OD): δ (ppm) 8.61 (t, 1H, J = 7.8 Hz, PyrH), 8.45 (d, 2H, J = 8.0 Hz, PyrH), 7.82 (d, 2H, J = 8.0 Hz, ArH), 7.24 (d, 2H, J = 7.8 Hz, ArH), 7.19 (s, 2H, ArH), 4.75 (q, 4H, J = 7.2 Hz, NCH_2), 1.28 (t, 6H, J = 7.2 Hz, CH_3). ^{13}C NMR (150.8, CD_3OD): δ (ppm) 156.3, 149.6, 141.5, 140.4, 131.3, 130.6, 127.1, 116.2, 113.2, 103.2, 50.8, 16.2. MS (MALDI): m/z 400.2 ($M+H^+$). HPLC: 14.0 min.

*General Procedure for the Preparation of **1** and **2**.* (D in Scheme 1) The appropriate phenolic derivative of **5** or **8** was added to a dry round-bottomed flask with the appropriate alkyl bromide or alkyl tosylate (5 equivalents), potassium carbonate (5 equivalents), and a 4:1 mixture of dry, degassed tetrahydrofuran and methanol (250 mM [Bip]). The reaction was refluxed at 75 °C for 12 h in an oil bath. The solvents were then removed in vacuo, and the dried solids were separated via extraction with DCM and water (3x 100 mL). The organic layers were combined and the solvent removed in vacuo. The following is an example of the characterization data for $\mathbf{1}^{Et4}$. Similar data for the additional derivatives of **1** and **2** are located in the Supporting Information.

2,6-Bis(5′-(n-buten-3″-yl-1-oxy)-1′-ethylbenzimidazol-2′-yl)pyridine ($\mathbf{1}^{Et4}$). Purified via column chromatography on silica ($CHCl_3$:MeOH 100:0 to 95:5) to yield the product as a white solid (78%). TLC (silica, 95:5 $CHCl_3$:MeOH) R_f = 0.29; mp: 120.3 °C. ^{1}H NMR (600 MHz, $CDCl_3$): δ (ppm) 8.31 (d, 2H, J = 7.8 Hz, PyrH), 8.02 (t, 1H, J = 8.1 Hz, PyrH), 7.35 (d, 2H, J = 8.4 Hz, ArH), 7.33 (d, 2H, J = 1.2 Hz, ArH), 7.03 (dd, 2H, J = 8.4, 1.2 Hz, ArH), 5.95 (m, 2H, $H_2C{=}CH$), 5.16 (dd, 4H, J = 40.2, 10.2 Hz, $H_2C{=}CH$), 4.78 (q, 4H, J = 7.2 Hz, NCH_2), 4.11 (t, 4H, J = 6.6 Hz, OCH_2), 2.61 (q, 4H, J = 6.6 Hz, OCH_2CH_2), 1.36 (t, 6H, J = 7.2 Hz, CH_3). ^{13}C NMR (150.8 MHz, $CDCl_3$): δ (ppm) 155.6, 149.8, 149.7, 143.4, 137.8, 134.4, 130.5, 125.2, 116.9, 114.5, 110.5, 102.8, 67.8, 39.8, 33.7, 15.6. MS (MALDI): m/z 508.9 ($M+H^+$). HPLC: 15.4 min.

ADMet Polymerizations. $\mathbf{1}^{Et5}$ or $\mathbf{1}^{Et5Me}$ and Grubbs catalyst third generation (5 mol %), were placed in a vial with a stir bar and dry, degassed DCM, which had been previously passed over basic alumina. The reaction was sealed with a septum and allowed to stir at room temperature for 3 h. During the first hour, argon was bubbled through the solution for 1 min every 10 min. The solvent was then removed in vacuo, and SEC analysis was performed on the crude material. For DSC and POM characterization, the crude reaction was purified via passing over a short plug of silica in DCM.

Formation of Metal Complexes. Equimolar amounts of the appropriate Bip derivative and metal salt were dissolved in dichloromethane and acetonitrile, respectively. These solutions were mixed, and the solvents removed in vacuo. The complexes were then redissolved in dichloromethane for purposes of casting films.

dx.doi.org/10.1021/cm2011617 |*Chem. Mater.* 2011, 23, 3525–3533

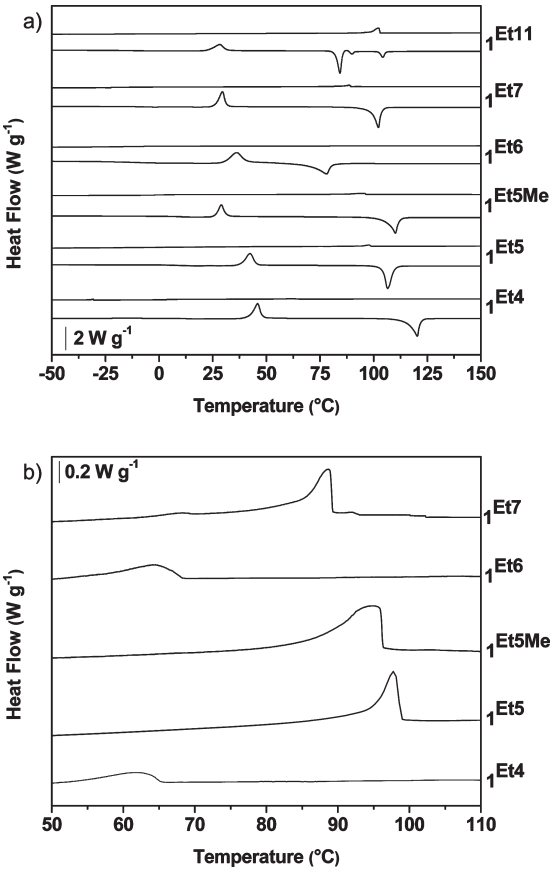

Figure 2. (a) DSC traces of the $\mathbf{1}^{Et}$ monomers and (b) expanded scale to reveal small exotherms upon cooling of $\mathbf{1}^{Et4}$, $\mathbf{1}^{Et5}$, $\mathbf{1}^{Et5Me}$, $\mathbf{1}^{Et6}$, and $\mathbf{1}^{Et7}$. Cooling traces are on top in panel (a) (exothermic up). Heating and cooling rate is 10 °C/min.

RESULTS AND DISCUSSION

Synthesis. Starting from commercially available materials, we prepared the acid chloride (**3**) and *o*-nitroaniline derivatives (**4**). These materials were subsequently reacted to yield **5** via methodology we recently reported.[10] The new class of mesogenic monomers (**1**) was prepared from **5** in two steps by deprotection of the aryl methoxy groups with BBr_3, followed by reaction of the appropriate halo-alkene with the resulting bis-phenol under Williamson ether synthesis conditions. The total synthesis of the Bip ligand derivatives (**1**) is carried out in five (or six for $\mathbf{1}^{Et5Me}$) steps from commercially available materials (Scheme 1) and allows access to the desired products in good overall yield (50−67%) and on a practical scale (>2 g). Using similar methodology, the synthesis of the aryl extended Bip derivatives (**2**), which feature a core with higher structural anisotropy,[10] requires one additional step from commercial materials (Scheme 1) but also allows access to the targeted species in similar yield (52−64%) on a practical scale.

Liquid Crystalline Properties of Derivatives of 1. Initially, our efforts concentrated on the series of Bip ligands based on core **1** with ethyl substituents on the nitrogen (1′-position, Figure 1) and linear alkenes ranging from four to eleven carbons in length on the 5′ oxygen ($\mathbf{1}^{Et}$, Scheme 1). The presence of thermal transitions indicative of liquid crystalline behavior in these materials was first investigated by differential scanning calorimetry (DSC) (Figure 2). The DSC traces reveal that each of these

Table 1. Selected Thermal Transitions of Monomers[a]

	transition	*T* (°C)	transition	*T* (°C)
$\mathbf{1}^{Et4}$	Cr → I	120.3	I → N	61.8
$\mathbf{1}^{Et5}$	Cr → I	106.5	I → N	97.7
$\mathbf{1}^{Et5Me}$	Cr → I	110.1	I → N	94.5
$\mathbf{1}^{Et6}$	Cr → I	78.1	I → N	64.0
$\mathbf{1}^{Et7}$	Cr → I	102.1	I → N	93.2
$\mathbf{1}^{Et7}$			N → S_C	72.2
$\mathbf{1}^{Et11}$	Cr → I	104.2	I → Cr	102.0
$\mathbf{2}^{Et5}$	Cr → I	216.4	I → Cr	159.3
$\mathbf{2}^{Bu5}$	Cr → I	178.4	I → N	150.2

[a] Transition temperatures taken from minima/maxima on DSC (mDSC for $\mathbf{1}^{Et7}$ cooling) heating/cooling traces. I-isotropic; N-nematic; S_C-smectic C; and Cr-Crystalline.

monomers undergoes a cold crystallization and melting upon heating, but that upon cooling, each derivative, except $\mathbf{1}^{Et11}$ (which features the longest alkene chains), exhibits a small exothermic transition rather than an obvious recrystallization exotherm. Consistent with what is observed in many other mesogenic systems the terminal olefins derivatives show a distinct odd/even effect in the temperature at which the isotropic to nematic transition occurs (Table 1). However, in this case the compounds with an even number of carbons on the alkyl chains exhibit a transition in the low 60s °C, while the odd carbon chain derivatives are much more stable exhibiting transitions in the mid 90s °C. This suggests that in this case the molecular anisotropy and hence molecular order is enhanced by having an odd number of carbons attached to the oxygen. Interestingly, $\mathbf{1}^{Et5Me}$, the derivative decorated with six carbon nonterminal olefins, behaves similarly to $\mathbf{1}^{Et5}$ rather than $\mathbf{1}^{Et6}$, suggesting that the location of the alkene within the chain has a greater effect on thermal behavior than the additional methyl unit. Thus, it appears that the alkene in the side chains of the mesogens may play an important role in the stabilizing interactions between these units. Also of note is that each of these monomers exhibits a T_g between −9.8 and 11.7 °C. As these materials vitrify below room temperature, they will exhibit liquid crystalline fluidity at useful temperatures. Although it should be noted that all the monomers are monotropic, exhibiting liquid crystallinity only upon cooling. The DSC trace of $\mathbf{1}^{Et11}$ shows a cold crystallization peak and three endothermic transitions observed upon heating. The POM of this material shows no observable change until it melts at 104.5 °C, which corresponds to the last of the three endotherms. At this point, we have no explanation for the other two endotherms at 87.2 and 90.1 °C other than the existence of solid−solid phase transitions. Upon cooling, it does show the expected recrystallization exotherm (102.0 °C), likely due to the significant length (11 carbons) of the alkene chains enhancing crystallization (Figure 2.)

To further probe the smaller transitions on cooling and determine if they are, in fact, evidence of the formation of liquid crystalline phases in these monomers, polarized light optical microscopy (POM) studies were performed on each ligand. Upon heating through the melting points determined by DSC, the micrographs showed the removal of birefringence to a dark state, consistent with an isotropic, liquid-like phase. Subsequent cooling through the temperature of the small transition observed in the DSC cooling traces, however, yielded a distinct Schlieren-like texture in the micrographs for $\mathbf{1}^{Et4}$, $\mathbf{1}^{Et5}$, $\mathbf{1}^{Et5Me}$, and $\mathbf{1}^{Et6}$, suggestive of a nematic liquid crystalline phase (Supporting

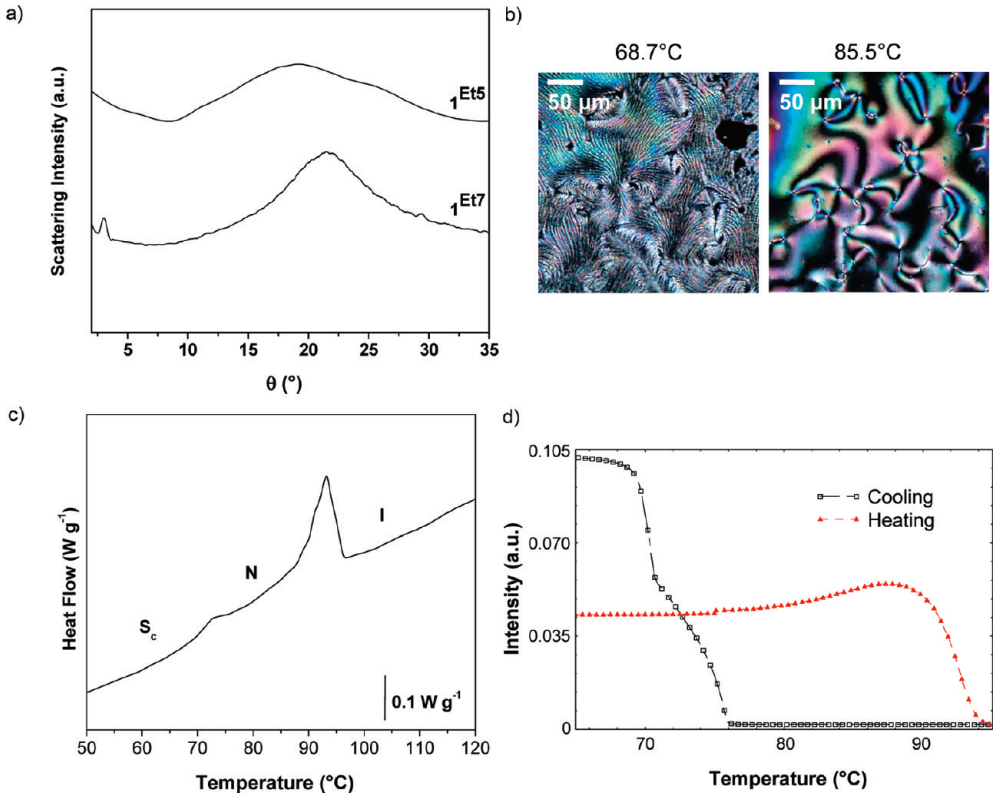

Figure 3. (A) WAXS of $\mathbf{1}^{Et5}$ (top trace) and $\mathbf{1}^{Et7}$ (bottom trace) after cooling to room temperature from the isotropic state at 10 °C/min, revealing only an amorphous halo in the former and a small peak consistent with a smectic arrangement in the latter. (b) POM images showing the birefringent textures of $\mathbf{1}^{Et7}$ upon cooling from isotropic to nematic and nematic to smectic states. (c) Modulated DSC thermogram (exothermic up) of the overall heat flow revealing two small exothermic transitions upon cooling (93.2 and 72.6 °C). (d) Temperature dependence of the transmitted light intensity through a 5 μm thick film of $\mathbf{1}^{Et7}$ with antiparallel rubbed polyimide coating for planar alignment integrated over about 1 mm^2 area. The polyimide thickness is roughly 50 nm.

Information). POM images taken below T_g confirm that this phase remains intact upon further cooling in each sample.

Wide-angle X-ray scattering (WAXS) experiments support the hypothesis that the transitions exhibited upon cooling in the DSC and POM data are from an isotropic phase to a more ordered nematic liquid crystalline phase. For example, the diffraction pattern of the powdered monomer $\mathbf{1}^{Et5}$ before any thermal treatment shows an array of reflections consistent with a crystalline solid, while upon heating, only an amorphous halo is visible. Cooling the sample again past the transition at 97.7 °C does not initially yield the return of crystalline reflections but rather the presence of a broad amorphous peak and the absence of long-range order, again in agreement with a nematic liquid crystalline material (Figure 3a, top). After several minutes at room temperature, ordered reflections begin to develop as the material crystallized, aided by the T_g of the material being below room temperature (about 9.5 °C). Crystallization was complete by WAXS after about 80 min at room temperature (Supporting Information). WAXS and POM experiments performed on the heptene-functionalized monomer ($\mathbf{1}^{Et7}$) showed a more complex behavior (Figure 3). As before, the POM micrographs show the absence of birefringence upon heating through the melting temperature observed by DSC (102.1 °C). Upon cooling through the small DSC exotherm (93.2 °C), a Schlieren-like texture appears, akin to that observed in the other monomers. Further cooling, however, reveals a fan-like texture, consistent with a smectic liquid crystalline phase (Figure 3b). Modulated DSC (mDSC, Figure 3c) was performed on the $\mathbf{1}^{Et7}$ monomer near the temperature of the change in texture observed during POM. Gratifyingly, this more sensitive technique revealed a second exotherm (72.6 °C) at a lower temperature than the first, consistent with the transition observed by POM. The presence of two liquid crystalline phases upon cooling was further supported by the measurement of the light intensity transmitted through a 5 μm thick sample placed between crossed polarizers. At a cooling rate of 1 °C/min, a double transition is observed at 75.5 and 70.6 °C. The liquid crystalline phase is still visible via this technique upon further cooling to room temperature (Figure 3d).

Electric current measurements on $\mathbf{1}^{Et7}$ indicated a somewhat ionic dielectric response. The dielectric measurements in the planar alignment cell show very low dielectric constant (barely above the square of the refractive index), except for the 1/frequency-type decrease, which is due to the dc conductivity that increases upon heating. The very low dielectric constant normal to the electric fields in the nematic phase is lower than the dielectric constant in the isotropic phase, which shows that the material has a positive dielectric anisotropy. This may indicate that the most stable conformation is not the bent-shaped *cis*/*cis*, but rather the more linear *trans*/*trans* conformation (Figure 1), as is observed in the crystal structure of similar Bip derivatives,[9a] or that the arms are twisted with respect to each other.

WAXS experiments (Figure 3a) were then carried out to determine if the final liquid crystalline phase upon cooling was,

dx.doi.org/10.1021/cm2011617 |*Chem. Mater.* 2011, 23, 3525–3533

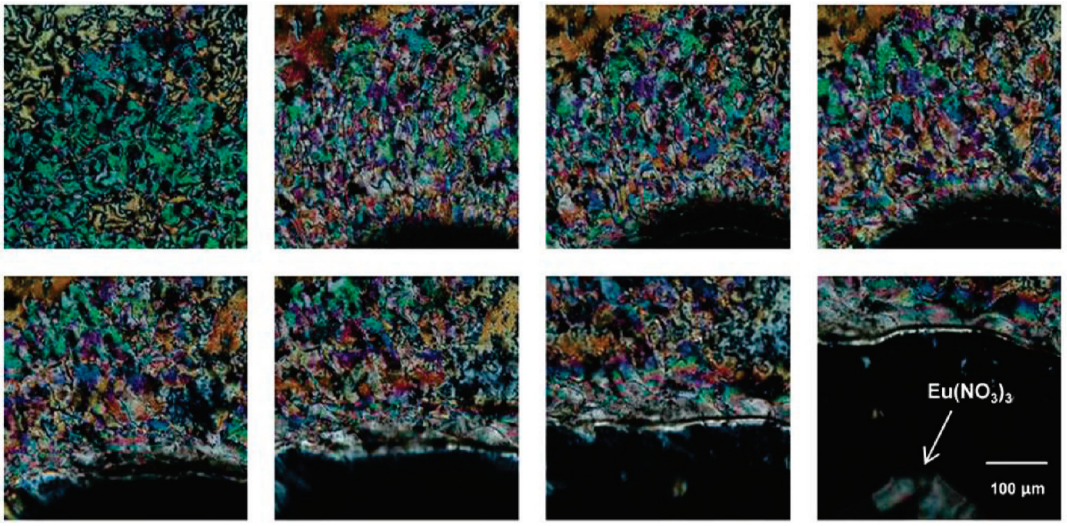

Figure 4. POM images displaying the optical response of $\mathbf{1}^{\mathbf{Et5}}$ with $Eu(NO_3)_3 \cdot 6H_2O$ at 95 °C. Top left image is the initial state. The next six images depict the advancing front of $Eu(NO_3)_3$ over 60 s. Bottom right image was repositioned to show the $Eu(NO_3)_3$ crystal.

in fact, a smectic phase. A reflection was indeed observed (about 29.3 Å), which corresponds to a distance slightly less than that of the energy minimized end-to-end distance (34.7 Å) of $\mathbf{1}^{\mathbf{Et7}}$ in its extended *trans* configuration. The location of this peak is consistent with the presence of a smectic C phase with a tilt angle of approximately 32° from normal (Supporting Information). We hypothesize that the longer alkene chains used to decorate $\mathbf{1}^{\mathbf{Et7}}$ compared to those on the other $\mathbf{1}^{\mathbf{Et}}$ ligands induce enhanced two-dimensional order, and thus upon cooling this monomer adopts a smectic arrangement after passing through a nematic region. As with the $\mathbf{1}^{\mathbf{Et5}}$ derivative, $\mathbf{1}^{\mathbf{Et7}}$ also has a T_g below room temperature (about −8.0 °C) and is also metastable, crystallizing over a period of days at room temperature.

Cognizant of the prior work by Piguet and co-workers,[11−14] and by the fact that we are interested in accessing polymeric liquid crystalline Bip compounds, where solubility can be an issue at higher degrees of polymerization, we were curious about what potential effects that increasing the length of the alkyl substituents in the $N^{1'}$ positions would have on the liquid crystalline behavior of our monomers. To that end, we synthesized derivatives with *n*-propyl, *n*-butyl, and *n*-hexyl chains in the $N^{1'}$ positions and pentene chains in the 5′ positions ($\mathbf{1}^{\mathbf{Pr5}}$, $\mathbf{1}^{\mathbf{Bu5}}$, $\mathbf{1}^{\mathbf{Hx5}}$). The *n*-butyl functionalized derivative was also prepared with a heptene chain in the 5′ positions ($\mathbf{1}^{\mathbf{Bu7}}$). While none of these monomers displayed liquid crystalline behavior, presumably due to changes in the aspect ratio of the monomer, their facile synthesis bodes well for both enhancing the solubility and tuning liquid crystalline properties of polymeric derivatives through copolymerization and/or blending with the mesogenic derivatives.

Liquid Crystalline Properties of Derivatives of 2. In addition to easily tuning the length of the $N^{1'}$ and 5′ alkyl/alkenyl substituents on these monomers, our synthetic scheme allows for the preparation of larger aromatic cores by introducing a phenyl ring between the Bip ligand and the 5′-substituent (**2**, Scheme 1). To probe potential liquid crystalline properties of these "extended" monomers, derivatives with ethyl and *n*-butyl chains on the $N^{1'}$ positions and pentene chains on the 5′ oxygen ($\mathbf{2}^{\mathbf{Et5}}$ and $\mathbf{2}^{\mathbf{Bu5}}$) were also prepared. These derivatives have a significantly larger aromatic surface, and as such, it was anticipated that they would be generally more crystalline than their "short" counterparts. DSC and POM experiments suggest that $\mathbf{2}^{\mathbf{Et5}}$ is, in fact, highly crystalline with a melting point of 216.4 °C (c.f. 106.5 °C for the related "short" derivative, $\mathbf{1}^{\mathbf{Et5}}$). The *n*-butyl functionalized derivative, however, displays different behavior. By increasing the length of the alkane chains at the $N^{1'}$ position, liquid crystalline order can be observed. DSC experiments reveal that upon heating $\mathbf{2}^{\mathbf{Bu5}}$ melts at 178.4 °C and upon cooling exhibits a small exotherm at 150.2 °C (c.f. the shorter $\mathbf{1}^{\mathbf{Bu5}}$ is an oil). POM micrographs taken at temperatures near this exotherm suggest a transition from an isotropic melt to a nematic liquid crystalline phase (see Supporting Information for DSC and POM data of **2**). These derivatives offer the option to incorporate crystalline or high-temperature liquid crystalline monomers into polymers, copolymers, blends, and networks, further enhancing the tunability of our design (Table 1).

Chemo-Response with Metal Salts. As part of our project to develop metallo-responsive liquid crystalline materials, we initially targeted mesogens that would become isotropic upon binding metal ions. It has been demonstrated[9−14] that Bip ligands bind to a variety of metal ions; thus, we carried out experiments to investigate the effects of this binding on the liquid crystalline behavior of these mesogens. Initial DSC and POM results have shown that addition of one equivalent of $Eu(NO_3)_3$ (which has been shown to form a 1:1 complex with Bip ligands)[31] to $\mathbf{1}^{\mathbf{Et5}}$ results in the switching of the system from nematic to isotropic.[10] Additional experiments (Supporting Information) suggest that this system becomes isotropic after exposure to only ∼0.6 equivalents of $Eu(NO_3)_3$. In a more direct demonstration of the metallo-response itself, a slide of $\mathbf{1}^{\mathbf{Et5}}$ was prepared, thermally treated as outlined above to yield a liquid crystalline phase, and then observed via POM as a crystal of $Eu(NO_3)_3 \cdot 6H_2O$ (mp: 40 °C) was placed upon the sample. Subsequent micrographs depict the advancing front of the molten metal salt as a border between birefringent (liquid crystalline) and dark (isotropic) regions (Figure 4). Similar isotropic behavior was observed when complexes of $\mathbf{1}^{\mathbf{Et5}}$ or $\mathbf{1}^{\mathbf{Et5Me}}$ were prepared with $Eu(ClO_4)_3$ (known to bind Bip derivatives in a 1:3 ratio), $Cu(OTf)_2$, and $Zn(OTf)_2$, which bind in 1:2 metal:ligand ratios.[25]

Polymerization via Acyclic Diene Metathesis (ADMet). As we are interested in accessing metallo-responsive polymers, we

have also investigated the ADMet polymerization (Scheme 2) of these monomers. Several attempts to polymerize $\mathbf{1}^{Et5}$ using a variety of documented metathesis conditions and catalysts yielded only oligomeric species with a maximum average degree of polymerization (DP) of 3.5 with specific short oligomers discernible via SEC (Figure 5a). Having ruled out other potential issues such as binding of the catalyst by the ligand and reduced solubility of the oligomers, we investigated that the possibility of side reactions occurring from decomposition products of the catalyst. Grubbs and co-workers published an elegant explanation of (and solution to) this problem whereby the formation of degradation products of the catalyst is hindered by using substrates with nonterminal olefins.[32] Thus, we attempted to polymerize $\mathbf{1}^{Et5Me}$ via the same method as above and were able to access a polymer of DP = 25 ($M_n \sim 14000$ g/mol, PDI = 2.5) by SEC (Figure 5a). It should be noted that because of the metathesis mechanism, $\mathbf{1}^{Et5}$ and $\mathbf{1}^{Et5Me}$ yield essentially the same polymer structure, with the former releasing ethylene and the latter butylene (Scheme 2).

Scheme 2. ADMet Polymerization of $\mathbf{1}^{Et5}$ and $\mathbf{1}^{Et5Me}$ to Yield Oligomeric and Polymeric Liquid Crystalline Materials

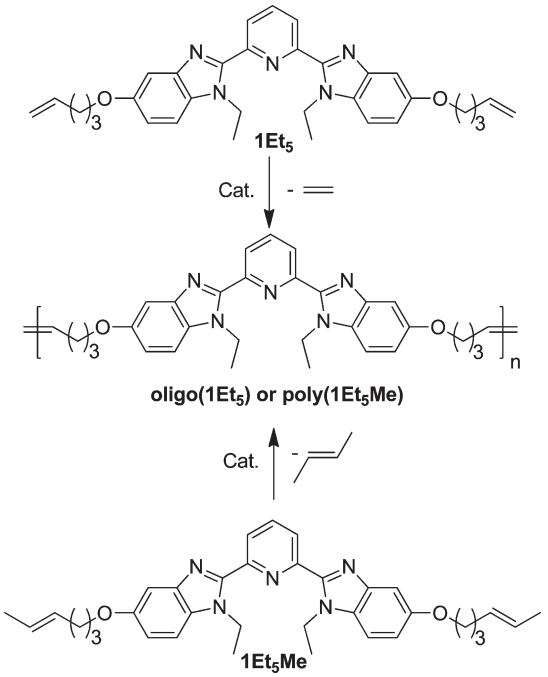

Having now successfully prepared both polymers and oligomers of $\mathbf{1}^{Et5}$, we then investigated their thermal properties. Thermal and optical analysis of oligo($\mathbf{1}^{Et5}$) revealed evidence of liquid crystalline behavior that differs significantly from that of the monomer. For example, unlike the monomer, which is metastable and monotropic (only exhibits liquid crystalline phases on cooling), DSC experiments (Figure 5b, top pair) suggest that the oligomer exhibits enantiotropic behavior, with transitions on heating that appear to correspond to a T_g at 65 °C and a clearing point at 155 °C. POM images (Figure 5c, left) taken in the temperature ranges suspected of liquid crystalline behavior reveal textures indicative of slightly smaller liquid crystalline domains than the monomer, as would be expected for a higher molecular weight molecule. This trend in smaller domain size appears to continue with poly($\mathbf{1}^{Et5Me}$), where a grainy birefringent texture is observed in the POM (Figure 5c, right), while the DSC traces (Figure 5b, bottom pair) show no discernible liquid crystalline transitions for this material over the observed temperature range (−90 to 200 °C).We suspect that the higher molecular weight polymer degrades before reaching its liquid crystalline to isotropic clearing temperature. We ascribe the dramatic differences in the LC behavior of the monomers and

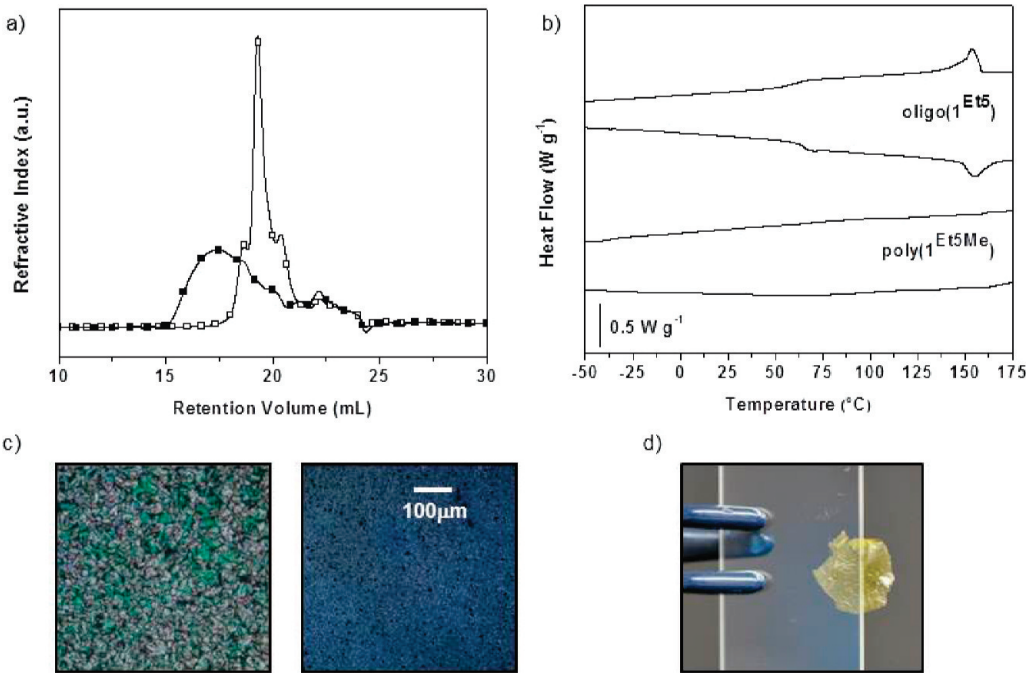

Figure 5. (a) SEC traces of oligo($\mathbf{1}^{Et5}$) (□) and poly($\mathbf{1}^{Et5Me}$) (■). (b) DSC traces of oligo($\mathbf{1}^{Et5}$) (top pair) and poly($\mathbf{1}^{Et5Me}$) (bottom pair) (cooling traces on top and exothermic up). (c) POM micrographs of oligo($\mathbf{1}^{Et5}$) (left image T = 135 °C) and poly($\mathbf{1}^{Et5Me}$) (right image T = 209 °C). (d) Film of poly($\mathbf{1}^{Et5Me}$) cross-linked with $Cu(OTf)_2$.

dx.doi.org/10.1021/cm2011617 |*Chem. Mater.* 2011, 23, 3525–3533

the oligomers or polymers at least in part to the reduced crystallinity of the polydispersed oligomers and polymers. The higher thermal stability of the LC phases in the polymer can also be ascribed to multivalent interactions between the mesogens within the polymer chain stabilizing the LC order. The addition of $Eu(NO_3)_3$ to poly($\mathbf{1}^{Et5Me}$) disrupts the liquid crystalline behavior, akin to that observed in the monomer, demonstrating that the polymer retains the metallo-responsive characteristics of the monomer. Interestingly, addition of a small amount of metal ion (e.g., $Cu(OTf)_2$, 10:1 Bip:Cu) that can bind two Bip ligands and thus cross-link poly($\mathbf{1}^{Et5Me}$) not only disrupts the liquid crystallinity of the polymer but also results in free-standing films of the material after solution casting (Figure 5d). Such films are not accessible with either the metal-free polymer, a solid which displays no film-forming behavior, or the metal complexes of the monomers or oligomer.

CONCLUSIONS

We have prepared a series of easy-to-access and scalable Bip-containing monomers with chemo-responsive liquid-crystalline properties. The derivatives that display liquid crystalline transitions do so only upon cooling from the isotropic phase and are thus monotropic, with transition temperatures ($I \rightarrow N$, or $I \rightarrow N \rightarrow S_C$) ranging from 61.8 to 150.2 °C. Upon cooling to room temperature, the liquid crystallinity of these materials is metastable (T_g of these materials is below room temperature), and cold crystallization is observed over a number of hours to days. These monomers are chemo-responsive, in that addition of lanthanide (or transition metal) salts, disrupts their liquid-crystalline behavior, providing a potentially useful "on/off" switching scheme. The alkene moieties attached in the 5′ positions provide a synthetic handle via which metathesis polymerizations have been performed yielding enantiotropic liquid crystalline oligomers (oligo($\mathbf{1}^{Et5}$)) and polymers (poly($\mathbf{1}^{Et5Me}$)), with the degree of polymerization dictated by the nature of the terminal alkene. These oligomers/polymers are also metallo-responsive in a similar manner to their monomeric counterparts but are now enantiotropic and show a dramatically reduced tendency to crystallize relative to the monomer. Cross-linking the polymeric species can also be achieved with appropriate metal salts, yielding materials that can be prepared as free-standing films. These results demonstrate the ability to utilize these ligand containing monomers to access metallo-responsive polymers where the interaction between the Bip ligand and a metal ion can be used to switch on/off the response. We are currently building on these initial results to access other classes of metallo-responsive materials, e.g., such as metallo-responsive liquid crystalline elastomers. Furthermore, we have previously shown that the lanthanide−Bip interaction is responsive to light[24] and as well as phosphine oxide containing molecules (such as those found in pesticides and nerve gas agents)[22] opening the door for Bip-containing polymers to be utilized to access structurally dynamic polymers that are multiresponsive.[28]

ASSOCIATED CONTENT

Supporting Information. Synthetic details and characterization data of **1**-**2**, **4**-**8**, and the phenolic derivatives of **5** and **8**, exemplary ^1H NMR and ^{13}C NMR spectra and POM micrographs of **1**-**2**, WAXS of $\mathbf{1}^{Et5}$ and $\mathbf{1}^{Et7}$, DSC traces of **2**, and DSC and POM titrations of $\mathbf{1}^{Et5}$ with $Eu(NO_3)_3$. This material is available free of charge via the Internet at http://pubs.acs.org.

AUTHOR INFORMATION

Corresponding Author
*E-Mail: stuart.rowan@case.edu.

ACKNOWLEDGMENT

This material is based upon work supported by the National Science Foundation (CHE-0704026, DMR-0758631, and DMR-0964765) and MRI-0821515 (for the purchase of the MALDI-TOF/TOF). R.J.W. acknowledges support through the NASA Graduate Student Research Program (NNX08AY62H). K.A.B. acknowledges the support of a Graduate Research Fellowship from the National Science Foundation (DGE-0234629).

REFERENCES

(1) (a) Demus, D.; Goodby, J. W.; Gray, G. W.; Speiss, H.-W.; Vill, V. *Handbook of Liquid Crystals*; Wiley-VCH: Weinheim, 1998. (b) Gray, G. W. *Thermotropic Liquid Crystals*; Wiley: Chichester, 1987. (c) Warner, M.; Terentjev, E. M. *Liquid Crystal Elastomers*; Oxford University Press: New York, 2003.

(2) (a) Kato, T. *Science* **2002**, *295*, 2414–2418. (b) Kato, T.; Mizoshita, N.; Kishimoto, K. *Angew. Chem., Int. Ed.* **2006**, *45*, 38–68. (c) Kato, T.; Hirai, Y.; Nakaso, S.; Moriyama, M. *Chem. Soc. Rev.* **2007**, *36*, 1857–1867. (d) Sagara, Y.; Kato, T. *Angew. Chem., Int. Ed.* **2008**, *47*, 5175–5178. (e) Hirai, Y.; Babu, S. S.; Praveen, V. K.; Yasuda, T.; Ajayaghosh, A.; Kato, T. *Adv. Mater.* **2009**, *21*, 4029–4033. (f) Isoda, K.; Yasuda, T.; Kato, T. *Chem. Asian J.* **2009**, *4*, 1619–1625. (g) Sagara, Y.; Kato, T. *Nature Chem.* **2009**, *1*, 605–610. (h) Pal, S. K.; Agarwal, A.; Abbott, N. L. *Small* **2009**, *5*, 2589–2596.

(3) (a) Burnworth, M.; Rowan, S. J.; Weder, C. *Chem.—Eur. J.* **2007**, *13*, 7828–7836. (b) Piepenbrock, M.-O. M.; Lloyd, G. O.; Clarke, N.; Steed, J. W. *Chem. Rev.* **2010**, *110*, 1960–2004.

(4) Beller, M.; Bolm, C. *Transition Metals for Organic Synthesis*; Wiley-VCH: Weinheim, 2004.

(5) Creus, M.; Ward, T. R. *Org. Biomol. Chem.* **2007**, *5*, 1835–1844.

(6) (a) Curry, R. J.; Gillin, W. P. *Curr. Opin. Solid St. M.* **2001**, *5*, 481–486. (b) Kuriki, K.; Koike, Y.; Okamoto, Y. *Chem. Rev.* **2002**, *102*, 2347–2356. (c) Kido, J.; Okamoto, Y. *Chem. Rev.* **2002**, *102*, 2357–2368. (d) Bender, J. L.; Corbin, P. S.; Fraser, C. L.; Metcalf, D. H.; Richardson, F. S.; Thomas, E. L.; Urbas, A. M. *J. Am. Chem. Soc.* **2002**, *124*, 8526–8527. (e) Vermonden, T.; van Steenbergen, M. J.; Besseling, N. A. M.; Marcelis, A. T. M.; Hennink, W. E.; Sudhölter, E. J. R.; Cohen Stuart, M. A. *J. Am. Chem. Soc.* **2004**, *126*, 15802–15808. (f) Handl, H. L.; Gillies, R. J. *Life Sc.* **2005**, *77*, 361–371. (g) Lemonnier, J.-F.; Guénée, L.; Bernardinelli, G.; Vigier, J.-F.; Bocquet, B.; Piguet, C. *Inorg. Chem.* **2010**, *49*, 1252–1265.

(7) (a) Lockwood, N. A.; Mohr, J. C.; Ji, L.; Murphy, C. J.; Palecek, S. P.; de Pablo, J. J.; Abbott, N. L. *Adv. Funct. Mater.* **2006**, *16*, 618–624. (b) Govindaraju, T.; Bertics, P. J.; Raines, R. T.; Abbott, N. L. *J. Am. Chem. Soc.* **2007**, *129*, 11223–11231. (c) Lowe, A. M.; Bertics, P. J.; Abbott, N. L. *Anal. Chem.* **2008**, *80*, 2637–2645. (d) Sivakumar, S.; Wark, K. L.; Gupta, J. K.; Abbott, N. L.; Caruso, F. *Adv. Funct. Mater.* **2009**, *19*, 2260–2265. (e) Yang, K.-L.; Cadwell, K.; Abbot, N. L. *J. Phys. Chem. B* **2004**, *108*, 20180–20186.

(8) (a) Serrano, J. L. *Metallomesogens: Synthesis, Properties and Applications*; VCH: Weinheim, 1996. (b) Date, R. W.; Iglesias, E. F.; Rowe, K. E.; Elliot, J. M.; Bruce, D. W. *Dalton Trans.* **2003**, 1914–1931.

(9) (a) Nozary, H.; Piguet, C.; Tissot, P.; Bernardinelli, G.; Bünzli, J.-C. G.; Deschenaux, R.; Guillon, D. *J. Am. Chem. Soc.* **1998**, *120*, 12274–12288. (b) Yu, S. C.; Hou, S.; Chan, W. K. *Macromolecules* **1999**, *32*, 5251–5256. (c) Ceniceros-Gómez, A. E.; Ramos-Organillo, A.; Hernández-Díaz, J.; Nieto-Martínez, J.; Contreras, R.; Castillo-Blum, S. E. *Heteroat. Chem.* **2000**, *11*, 392–398. (d) Froidevaux, P.; Harrowfield, J. M.; Sobolev, A. N. *Inorg. Chem.* **2000**, *39*, 4678–4687. (e) Hasegawa, M.; Renz, F.; Hara, T.; Kikuchi, Y.; Fukuda, Y.; Okubo, J.; Hoshi, T.;

Linert, W. *Chem. Phys.* **2002**, *277*, 21–30. (f) Enamullah, M.; Linert, W. *Thermochim. Acta* **2002**, *388*, 401–406. (g) Haga, M.-A.; Takasugi, T.; Tomie, A.; Ishizuya, M.; Yamada, T.; Hossain, M. D.; Inoue, M. *Dalton Trans.* **2003**, 2069–2079. (h) Vaidyanathan, V. G.; Nair, B. U. *Eur. J. Inorg. Chem.* **2003**, 3633–3638. (i) Wang, X.; Wang, S.; Li, L.; Sundberg, E. B.; Gacho, G. P. *Inorg. Chem.* **2003**, *42*, 7799–7808. (j) Liu, S.-G.; Zuo, J.-L.; Li, Y.-Z.; You, X.-Z. *J. Mol. Struct.* **2004**, *705*, 153–157. (k) Xiao, L.; Zhang, H.; Jana, T.; Scanlon, E.; Chen, R.; Choe, E.-W.; Ramanathan, L. S.; Yu, S.; Benicewicz, B. C. *Fuel Cells* **2005**, *5*, 287–295. (l) Kanehara, M.; Kodzuka, E.; Teranishi, T. J. *J. Am. Chem. Soc.* **2006**, *128*, 13084–13094. (m) Yue, S.-M.; Xu, H.-B.; Ma, J.-F.; Su, Z.-M.; Kan, Y.-H.; Zhang, H.-J. *Polyhedron* **2006**, *25*, 635–644. (n) Chetia, B.; Iyer, P. K. *Tetrahedron Lett.* **2006**, *47*, 8115–8117. (o) Haga, M.-A.; Kobayashi, K.; Terada, K. *Coord. Chem. Rev.* **2007**, *251*, 2688–2701.

(10) McKenzie, B. M.; Miller, A. K.; Wojtecki, R. J.; Johnson, J. C.; Burke, K. A.; Tzeng, K. A.; Mather, P. T.; Rowan, S. J. *Tetrahedron* **2008**, *64*, 8488–8495.

(11) (a) Nozary, H.; Piguet, C.; Tissot, P.; Bernardinelli, G.; Deschenaux, R.; Vilches, M.-T. *Chem. Commun.* **1997**, 2101–2102. (b) Nozary, H.; Piguet, C.; Rivera, J.-P.; Tissot, P.; Bernardinelli, G.; Vulliermet, N.; Weber, J.; Bünzli, J.-C. G. *Inorg. Chem.* **2000**, *39*, 5286–5298. (c) Nozary, H.; Piguet, C.; Rivera, J.-P.; Tissot, P.; Morgantini, P.-Y.; Weber, J.; Bernardinelli, G.; Bünzli, J.-C. G.; Deschenaux, R.; Donnio, B.; Guillon, D. *Chem. Mater.* **2002**, *14*, 1075–1090.

(12) Nozary, H.; Piguet, C.; Tissot, P.; Bernardinelli, G.; Bünzli, J.-C. G.; Deschenaux, R.; Donnio, B.; Guillon, D. *J. Am. Chem. Soc.* **1998**, *120*, 12274–12288.

(13) (a) Terazzi, E.; Bénech, J.-M.; Rivera, J.-P.; Bernardinelli, G.; Donnio, B.; Guillon, D.; Piguet, C. *Dalton Trans.* **2003**, 769–772. (b) Terazzi, E.; Torelli, S.; Bernardinelli, G.; Rivera, J.-P.; Bénech, J.-M.; Bourgogne, C.; Donnio, B.; Guillon, D.; Imbert, D.; Bünzli, J.-C. G.; Pinto, A.; Jeannerat, D.; Piguet, C. *J. Am. Chem. Soc.* **2005**, *127*, 888–903. (c) Terazzi, E.; Suarez, S.; Torelli, S.; Nozary, H.; Imbert, D.; Mamula, O.; Rivera, J.-P.; Guillet, E.; Bénech, J.-M.; Bernardinelli, G.; Scopelliti, R.; Donnino, B.; Guillon, D.; Bünzli, J.-C. G.; Piguet, C. *Adv. Func. Mater.* **2006**, *16*, 157–168.

(14) Escande, A.; Guénée, L.; Nozary, H.; Bernardinelli, G.; Gumy, F.; Aebischer, A.; Bünzli, J.-C. G.; Donnio, B.; Guillon, D.; Piguet, C. *Chem.—Eur. J.* **2007**, *13*, 8696–8713.

(15) (a) Binnemans, K.; Görller-Warland, C. *Chem. Rev.* **2002**, *102*, 2303–2345. (b) Binnemans, K. *J. Mater. Chem.* **2009**, *19*, 448–453.

(16) Yelamaggad, C. V.; Prabhu, R.; Shanker, G.; Bruce, D. W. *Liq. Cryst.* **2009**, *36*, 247–255.

(17) Rowe, K. E.; Bruce, D. W. *J. Chem. Soc., Dalton Trans.* **1996**, 3913–3915.

(18) (a) Cardinaels, T.; Driesen, K.; Parac-Vogt, T. N.; Heinrich, B.; Bourgogne, C.; Guillon, D.; Donnio, B.; Binnemans, K. *Chem. Mater.* **2005**, *17*, 6589–6598. (b) Baranoff, E. D.; Voigner, J.; Yasuda, T.; Heitz, V.; Sauvage, J.-P.; Kato, T. *Angew. Chem., Int. Ed.* **2007**, *46*, 4680–4683. (c) Cardinaels, T.; Ramaekers, J.; Nockemann, P.; Driesen, K.; Van Hecke, K.; Van Meervelt, L.; Wang, G.; De Feyter, S.; Iglesias, E. F.; Guillon, D.; Donnio, B.; Binnemans, K.; Bruce, D. W. *Soft Matter* **2008**, *4*, 2172–2185. (d) Cardinaels, T.; Ramaekers, J.; Driesen, K.; Nockemann, P.; Van Hecke, K.; Van Meervelt, L.; Goderis, B.; Binnemans, K. *Inorg. Chem.* **2009**, *48*, 2490–2499.

(19) Holbrey, J. D.; Tiddy, G. J. T.; Bruce, D. W. *J. Chem. Soc., Dalton Trans.* **1995**, 1769–1774.

(20) (a) Bruce, D. W. *Acc. Chem. Res.* **2000**, *33*, 831–840. (b) Morale, F.; Date, R. W.; Guillon, D.; Bruce, D. W.; Finn, R. L.; Wilson, C.; Blake, A. J.; Schröder, M.; Donnio, B. *Chem.—Eur. J.* **2003**, *9*, 2484–2501. (c) Kozhevnikov, V. N.; Donnio, B.; Bruce, D. W. *Angew. Chem., Int. Ed.* **2008**, *47*, 6286–6289. (d) Santoro, A.; Whitwood, A. C.; Williams, J. A. G.; Kozhevnikov, V. N.; Bruce, D. W. *Chem. Mater.* **2009**, *21*, 3871–3882.

(21) (a) McKenzie, B. M.; Rowan, S. J. *The Encyclopedia of Supramolecular Chemistry*; Taylor and Francis: New York, 2007. (b) McKenzie, B. M.; Rowan, S. J. *Molecular Recognition and Polymers: Control of Polymer Structure and Self-Assembly*; Wiley: New York, 2008. (c) Fox, J. D.; Rowan, S. J. *Macromolecules* **2009**, *42*, 6823–6835.

(22) (a) Knapton, D.; Burnworth, M.; Rowan, S. J.; Weder, C. *Angew. Chem., Int. Ed.* **2006**, *45*, 5825–5829. (b) Kumpfer, J. R.; Jin, J.; Rowan, S. J. *J. Mater. Chem.* **2010**, *20*, 145–151.

(23) Beck, J. B.; Ineman, J. M.; Rowan, S. J. *Macromolecules* **2005**, *38*, 5060–5068.

(24) Burnworth, M.; Tang, L.; Kumpfer, J. R.; Duncan, A. J.; Beyer, F. L.; Rowan, S. J.; Weder, C. *Nature* **2011**, *472*, 334–338.

(25) (a) Beck, J. B.; Rowan, S. J. *J. Am. Chem. Soc.* **2003**, *125*, 13922–13923. (b) Zhao, Y.; Beck, J. B.; Rowan, S. J.; Jamieson, A. M. *Macromolecules* **2004**, *37*, 3529–3531. (c) Rowan, S. J.; Beck, J. B. *Faraday Discuss.* **2005**, *128*, 43–53. (d) Weng, W.; Beck, J. B.; Jamieson, A. M.; Rowan, S. J. *J. Am. Chem. Soc.* **2006**, *128*, 11663–11672. (e) Weng, W.; Jamieson, A. M.; Rowan, S. J. *Tetrahedron* **2007**, *63*, 7419–7431. (f) Weng, W.; Li, Z.; Jamieson, A. M.; Rowan, S. J. *Macromolecules* **2009**, *42*, 236–246. (g) Weng, W.; Li, Z.; Jamieson, A. M.; Rowan, S. J. *Soft Matter* **2009**, *5*, 4647–4657.

(26) (a) Knapton, D.; Iyer, P. K.; Rowan, S. J.; Weder, C. *Macromolecules* **2006**, *39*, 4069–4075. (b) Burnworth, M.; Knapton, D.; Rowan, S. J.; Weder, C. J. *Inorg. Organomet. Polym.* **2007**, *17*, 91–103.

(27) (a) Iyer, P. K.; Beck, J. B.; Weder, C.; Rowan, S. J. *Chem. Commun.* **2005**, 319–321. (b) Knapton, D.; Rowan, S. J.; Weder, C. *Macromolecules* **2006**, *39*, 651–657.

(28) Wojtecki, R. J.; Meador, M. A.; Rowan, S. J. *Nat. Mater.* **2011**, *10*, 14–27.

(29) For a recent review see: Opper, K. L.; Wagener, K.B. J. *Polym. Sci.: Part A: Polym. Chem.* **2011**, *49*, 821–831.

(30) Love, J. A.; Morgan, J. P.; Trnka, T. M.; Grubbs, R. H. *Angew. Chem., Int. Ed.* **2002**, *41*, 4035–4037.

(31) Piguet, C.; Williams, A. F.; Bernardinelli, G.; Moret, E.; Bünzli, J.-C. G. *Helv. Chim. Acta* **1992**, *75*, 1697–1717.

(32) (a) Hong, S. H.; Sanders, D. P.; Lee, C. W.; Grubbs, R. H. *J. Am. Chem. Soc.* **2005**, *127*, 17160–17161. (b) Hong, S. H.; Wenzel, A. G.; Salguero, T. T.; Day, M. W.; Grubbs, R. H. *J. Am. Chem. Soc.* **2007**, *129*, 7961–7968.